

BBA42619

## The effect of thylakoid membrane reorganisation on chlorophyll fluorescence lifetime components: a comparison between state transitions, protein phosphorylation and the absence of $\text{Mg}^{2+}$

M. Hodges, J.-M. Briantais and I. Moya

*Laboratoire de Photosynthèse, CNRS, Gif-sur-Yvette (France)*

(Received 2 February 1987)

**Key words:** Chlorophyll fluorescence lifetime; Excitation energy transfer; Photosynthesis; Protein phosphorylation; State transition; (*C. pyrenoidosa*)

Room temperature chlorophyll fluorescence lifetime measurements using single photon counting and low-intensity laser excitation have been carried out on photosynthetic systems which have undergone protein reorganisation by an in vivo state 1–state 2 transition, protein phosphorylation and the absence of  $\text{Mg}^{2+}$ . Analysis of the global changes in average lifetime and total fluorescence yield suggest that each treatment brings about a decrease in Photosystem (PS) II absorption cross-section but that this mechanism of energy redistribution accounts for different proportions of the total fluorescence quenching in the various cases. Further analysis of the overall fluorescence decay into individual kinetic components was carried out using a four-exponential model. The state transition did not alter the lifetimes of the four components but decreased the fluorescence yield of the long-lived decay, at both  $F_0$  and  $F_M$ , by 24% and increased the yield of the rapid components. Such changes infer that there is a decrease in PS II absorption cross-section and an increase in PS I excitation on going from state 1 to state 2. Furthermore, these alterations show that the 500 ps component (at  $F_0$ ) gives rise to the 2 ns decay (at  $F_M$ ). After in vitro protein phosphorylation at 5 mM  $\text{Mg}^{2+}$ , the changes are very similar to those brought about by a state transition, except that both long-lived kinetic components exhibit a decrease in yield. When protein phosphorylation was carried out at 2 mM  $\text{Mg}^{2+}$  a slight decrease in the lifetimes of the two slow components was observed, with a further decrease in the yield of the 2.3 ns decay and a larger increase in the yields of the two rapid decays. Although the fluorescence quenching brought about by the absence of  $\text{Mg}^{2+}$  (57%) was the largest of all the treatments, only a small part could be explained by a decrease in PS II absorption cross-section (17%). The absence of  $\text{Mg}^{2+}$  led to a decrease in the lifetimes and yields of the two long-lived decays. A careful comparison of the characteristics of the slowest component in the presence and absence of 5 mM  $\text{Mg}^{2+}$  on closing the PS II traps suggest that this decay has different origins in the two cases.

Chl, chlorophyll; PS, Photosystem; LHC, light-harvesting Chl *a/b* complex;  $Q_A$ , primary stable electron acceptor of PS II;  $F_M$ , maximum Chl fluorescence yield;  $F_0$ , initial Chl fluorescence yield;  $F_v$ , variable Chl fluorescence; DBMIB, 2,5-dibromo-3-methyl-6-isopropyl-*p*-benzoquinone; DCMU, 3-(3,4-dichlorophenyl)-1,1-dimethylurea.

Correspondence: M. Hodges, Laboratoire de Photosynthèse, CNRS, 91190 Gif-sur-Yvette, France.

### Introduction

The ability of oxygen-evolving photosynthetic organisms to regulate excitation energy distribution between the two photosystems to maintain maximal photosynthetic efficiency under varying light qualities was first demonstrated by Bona-

ventura and Myers [1] in 1969. The so-called state 1–state 2 transition is now a well-documented physiological mechanism found in a wide range of photosynthetic systems (see Ref. 2). Originally it was proposed that this process was controlled by light-induced ionic movements across the thylakoid membranes [3]. However, it is now well established that in LHC-containing photosynthetic systems the state transition involves the reversible phosphorylation of the LHC II [4–6]. Many workers have used the analysis of room temperature fluorescence induction curve kinetics in DCMU-inhibited thylakoids to investigate the mechanism of the redistribution of energy due to protein phosphorylation [7–9]. From such studies a cation dependence on the extent of the fluorescence quenching [8,9] and thylakoid reorganisation [10] was observed, as expected for a process under electrostatic control (see Ref. 2). It was concluded that at ‘saturating’ concentrations of cations (e.g., 10 mM  $\text{Mg}^{2+}$ ) phosphorylation led to a decrease in the absorption cross-section of PS II, while at ‘sub-saturating’ salt levels (e.g., no more than 2 mM  $\text{Mg}^{2+}$ ) an additional quenching was seen as a consequence of an increased spillover of excitation energy from PS II to PS I [9–11]. It is, however, still not clear if the *in vivo* state transition reflects the phosphorylation of LHC II at saturating or sub-saturating cation levels, and therefore if the change from state 1 to state 2 arises solely from a decrease in PS II absorption cross-section or from both changes in spillover and absorption cross-section. Although electron microscopy [12], fluorescence analyses [9,11,13] and photoacoustic measurements [14] favour the latter case, other reports in the literature have shown changes similar to those seen for the sub-saturating cation situation [15–17].

A direct method to distinguish between a change in absorption cross-section and other deactivation processes, like spillover and internal conversion (heat), brought about by state transitions, protein phosphorylation (see Refs. 18 and 19) or the absence of  $\text{Mg}^{2+}$  (see Refs. 20 and 21) is the analysis of room temperature chlorophyll fluorescence decay kinetics. Early work in this area, concerning the changes in excitation energy redistribution by the presence and absence of cations, was carried out by measuring the average lifetime and total

fluorescence yield of thylakoids, as the PS II reaction centres were closed to photochemistry, by the phase shift method [22]. This ‘global’ analysis gave valuable information concerning any differences in absorption cross-section by a change in the slope of the plot of average lifetime against total fluorescence yield. On this global level a decrease in the PS II absorption cross-section would be expected to change only the fluorescence yield ( $\phi$ ) and not the average lifetime ( $\tau$ ), whereas an increase in spillover would decrease both yield and average lifetime.

Recent studies, using a combination of single photon counting and low intensity picosecond laser excitation, have revealed the extreme complexity of the overall fluorescence decay (see Refs. 23 and 24); however, as for the ‘global’ level, a change in absorption cross-section will only change the yield of an emission while a change in non-radiative decay processes will decrease both yield and lifetime. Our results suggest that in the intact system it is possible to analyse the overall decay in terms of four exponential components [25]. By using a reductionist approach (involving mutants, isolated pigment-protein complexes and PS II-enriched membranes) it has been shown that variable chlorophyll fluorescence arises from three PS II-associated emissions while there exists two minor constant, rapid (less than 200 ps) PS I-associated emissions [26]. This means that the above-mentioned ‘global’ analysis is still valid, although the overall decay is heterogeneous in nature because all of the variable fluorescence arises from three components which exhibit a proportionality between lifetime and yield [26]. Other workers suggest the presence of only three decay components arising from PS I (80 ps), PS II $\alpha$  (200 ps at  $F_0$  and 2 ns at  $F_M$ ) and PS II $\beta$  (500 ps at  $F_0$  and 1 ns at  $F_M$ ) [24,27].

In this work we investigate and compare the changes in fluorescence lifetime and yield, on both the global and individual component level, brought about by state transitions in intact algae and protein phosphorylation and the absence of  $\text{Mg}^{2+}$  in isolated higher plant thylakoids. The analysis of dinitrobenzene quenching on the steady-state fluorescence level exhibited by state 1 and state 2 adapted algae is also investigated. The aim of this work is to examine the mechanisms involved in

excitation energy redistribution in the three different cases, to see if the state transition involves the phosphorylation of LHC II at 'high' or 'low' salt levels and to gain further information concerning the origins of the different decay components.

## Materials and Methods

Intact chloroplasts were prepared from either market lettuce or greenhouse peas as described in Ref. 28 and resuspended as a concentrated stock in a medium containing 0.33 M sorbitol (pH 7.5, Tris) and 5 mM  $\text{MgCl}_2$ . *Chlorella pyrenoidosa* were grown as described in Ref. 29.

Adaptation to either state 1 or state 2 was carried out using intact *C. pyrenoidosa* cells diluted in the growth medium to 20  $\mu\text{g}$  Chl/ml. State 1 was produced by illuminating the algae with far red light (Balzer 706 nm interference filter) at an intensity of 20  $\text{W} \cdot \text{m}^{-2}$  for 15 min. State 2 was generated by illuminating the algae, in the presence of 10 mM NaF, with green light (Corning filters 4-96 and 3-69) at an intensity of 10  $\text{W} \cdot \text{m}^{-2}$  for 15 min. Protein phosphorylation was carried out using pea thylakoids in the presence of either 5 or 2 mM  $\text{MgCl}_2$  as described elsewhere [9], using *Spirulina maxima* ferredoxin and NADPH to activate the kinase. The effect of  $\text{Mg}^{2+}$  was investigated by resuspending shocked lettuce chloroplasts in the presence or absence of 5 mM  $\text{MgCl}_2$  as described in Ref. 11.

Room temperature chlorophyll fluorescence lifetime measurements were carried out and analysed using the criteria and apparatus described in Ref. 29. Room temperature fluorescence induction curves were measured at 2  $\mu\text{g}$  Chl/ml using the apparatus described in Ref. 30 and green light at 15  $\text{W} \cdot \text{m}^{-2}$ . Titration of chlorophyll fluorescence with dinitrobenzene was carried out by the sequential addition of 30  $\mu\text{M}$  dinitrobenzene to continually stirred algae, adapted to state 1 or state 2, in the presence of 20  $\mu\text{M}$  DCMU. Steady-state fluorescence was measured at room temperature by illuminating the algae with green light at an intensity of 20  $\text{W} \cdot \text{m}^{-2}$ . The resulting signal was transmitted to a photomultiplier, via a fibre optic guide system, protected by a 670 nm cut-off filter (RG5). The changes in the fluorescence yield were analysed as described in Ref. 11.

## Results

Phosphorylation was checked by measuring and analysing room temperature fluorescence induction curves in DCMU-poisoned thylakoids. As previously reported [9], at 5 mM  $\text{Mg}^{2+}$  the phosphorylation treatment led to a proportional decrease in the  $F_0$  and  $F_M$  levels (15–25%), an increase in the  $t_{1/2}$  of the  $F_V$  (15–25%) and a slight reduction in the curvature of the plot  $F_V$  versus area over the curve. The absence of  $\text{Mg}^{2+}$  gave rise to an exponential fluorescence rise and an almost linear relationship between  $F_V$  and area (proportional to  $Q_A$  redox state) (data not shown).

Fig. 1 shows the effect of a state 1–state 2 transition (A) and protein phosphorylation at 5 mM  $\text{Mg}^{2+}$  (B) on the relationship between average lifetime and total fluorescence yield as a function of different degrees of PS II trap closure. The same type of plot is shown in Fig. 2 in the absence and presence of 5 mM  $\text{Mg}^{2+}$ . Table I gives the percentage change in the slope of the best fit to the datum points ( $\alpha$ ), the average lifetime ( $\tau_{\text{mean}}$ ) and the fluorescence yield ( $\phi_T$ ) for the different treatments represented in Figs. 1 and 2 as well as the values for thylakoids phosphorylated at 2 mM  $\text{Mg}^{2+}$  (plot not shown). It can be seen that in each case there is a diminution in the absorption cross-section of PS II (as seen from  $\alpha$ ), but this change reflects a different proportion of the total fluorescence quenching for the various situations. From

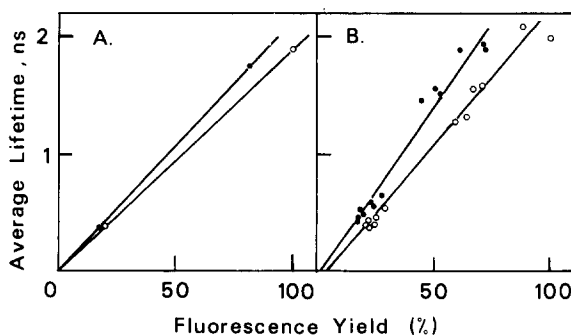


Fig. 1. The effect of (A) state transition in *C. pyrenoidosa* ( $\circ$ , state 1;  $\bullet$ , state 2) and (B) protein phosphorylation at 5 mM  $\text{Mg}^{2+}$  in pea thylakoids ( $\circ$ , nonphosphorylated;  $\bullet$ , phosphorylated) on the average lifetime (ns) as a function of total chlorophyll fluorescence yield (% of  $F_M$  in either state 1 (A) or nonphosphorylated protein (B)).

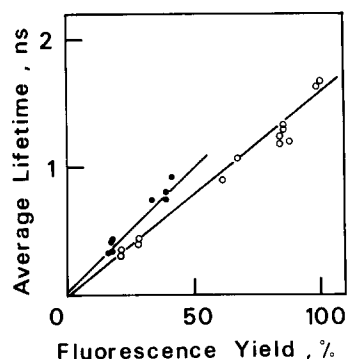


Fig. 2. The effect of the presence of 5 mM  $\text{Mg}^{2+}$  (○) and the absence of  $\text{Mg}^{2+}$  (●) on the average lifetime (ns) as a function of the total fluorescence yield (% of  $F_M$  plus  $\text{Mg}^{2+}$ ) in lettuce thylakoids.

this global analysis the fluorescence quenching by the state transition appears to be mainly due to a decrease in PS II absorption cross-section, whereas whereas this mechanism can account for all of the fluorescence change brought about by phosphorylation at 5 mM  $\text{Mg}^{2+}$ . In these two situations there is only a very small change in the average lifetime. At 2 mM  $\text{Mg}^{2+}$  the phosphorylation does not significantly alter the decrease in PS II absorption cross-section seen after phosphorylation at 5 mM  $\text{Mg}^{2+}$ , but produces an additional quenching which decreases the  $\tau_{\text{mean}}$ . In the absence of  $\text{Mg}^{2+}$  most of the 57% decrease in fluorescence yield appears to be due to changes in energy transfer which affect  $\tau_{\text{mean}}$ , with only a

TABLE I

THE EFFECT OF A STATE 1-STATE 2 TRANSITION, PROTEIN PHOSPHORYLATION AT 5 AND 2 mM  $\text{Mg}^{2+}$  AND CATION ( $\text{Mg}^{2+}$ ) DEPLETION ON THE TOTAL FLUORESCENCE YIELD ( $\phi_T$ ), AVERAGE LIFETIME ( $\tau_{\text{mean}}$ ) AND ABSORPTION CROSS-SECTION ( $\alpha$ ) AT  $F_M$ .

$\alpha$  is the fraction of incident light absorbed by PS II and is proportional to the inverse of the slope of the  $\tau_{\text{mean}} - \phi_T$  relationship depicted in Figs. 1 and 2.

	State transition	Phosphorylation		Cation
		5 mM $\text{Mg}^{2+}$	2 mM $\text{Mg}^{2+}$	
- $\Delta\phi_T$	18	27	47	57
- $\Delta\tau_{\text{mean}}$	8	5	21	48
- $\Delta\alpha$	13	26	30	17

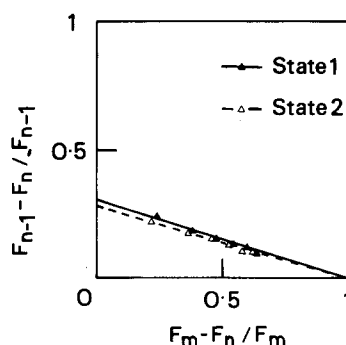


Fig. 3. Titration of the  $F_M$  exhibited by *C. pyrenoidosa* in either state 1 (▲) or state 2 (△) with sequential additions of 30  $\mu\text{M}$  dinitrobenzene. The lines are the least-squares fit to all of the experimental datum points with a regression coefficient ( $r$ ) = 0.99 for both cases.

small proportion of the decrease arising from a lowering of the PS II absorption cross-section.

Fig. 3 shows the titration of the total chlorophyll fluorescence, by sequential additions of dinitrobenzene, on intact *C. pyrenoidosa* cells pre-adapted to either state 1 or state 2. Similar titrations using DBMIB (which does not enter rapidly into intact cells) have already been carried out in phosphorylated thylakoids [31] at different background cation concentrations [11]. The y-intercept, at  $(F_M - F_n)/F_M = 0$ , where  $F_n$  is the fluorescence level after  $n$  additions of dinitrobenzene, gives a value which is directly proportional to the extent of the interaction between the dinitrobenzene and the fluorescing PS II pigments, and for convenience is termed the interaction index, as discussed in Ref. 31, from which the method of analysis is taken. It can be seen that on going from state 1 to state 2 the interaction index changes from 0.30 to 0.28 (a decrease of 6.7%), indicating that there is only a very small increase in the competition between dinitrobenzene and the 'normal' deactivation processes.

Table II gives the lifetimes ( $\tau_c$ ), amplitudes ( $A_{\text{exp}}$ ) and the fluorescence yields ( $\phi_c$ ) for the individual decay components exhibited by state 1 and state 2 adapted *C. pyrenoidosa* at  $F_0$  and  $F_M$ . A state 2-induced quenching of chlorophyll fluorescence can be seen at both fluorescence levels. At  $F_0$  the overall decay was deconvoluted in terms of only three decay components and it can be seen that the  $\tau_c$  values were not affected by the state

TABLE II

COMPONENT LIFETIME (ns), AMPLITUDE ( $A_{\text{exp}}$  (%)) AND FLUORESCENCE YIELD (REL. UNITS), AVERAGE LIFE-TIME ( $\tau_{\text{mean}}$  (ns)) AND TOTAL FLUORESCENCE YIELD (REL. UNITS) EXHIBITED BY *C. PYRENOIDOSA* IN STATE 1 AND STATE 2 AT  $F_0$  AND  $F_M$ .

Condition	Component characteristics					$\tau_{\text{mean}}$ $\phi_T$
$F_0$						
State 1						
$\tau_c$	—	0.500	0.212	0.041		0.387
$A_{\text{exp}}$	—	0.31	0.32	0.37		—
$\phi_c$	—	12.3	5.3	1.2		18.8
State 2						
$\tau_c$	—	0.487	0.208	0.038		0.364
$A_{\text{exp}}$	—	0.26	0.34	0.40		—
$\phi_c$	—	10.2	5.6	1.2		17.0
$F_M$						
State 1						
$\tau_c$	2.093	1.092	0.310	0.070		1.898
$A_{\text{exp}}$	0.47	0.16	0.11	0.26		—
$\phi_c$	79.2	13.9	2.8	1.44		97.4
State 2						
$\tau_c$	2.014	1.080	0.278	0.071		1.744
$A_{\text{exp}}$	0.36	0.16	0.14	0.34		—
$\phi_c$	60.6	14.4	3.3	2.0		79.9

TABLE III

COMPONENT LIFETIME (ns), AMPLITUDE ( $A_{\text{exp}}$  (%)) AND FLUORESCENCE YIELD (REL. UNITS), AVERAGE LIFE-TIME ( $\tau_{\text{mean}}$  (ns)) AND TOTAL FLUORESCENCE YIELD (REL. UNITS) EXHIBITED BY NONPHOSPHORYLATED AND PHOSPHORYLATED PEA CHLOROPLASTS AT 5 AND 2 mM  $\text{Mg}^{2+}$  AT  $F_M$

Condition	Component characteristics					$\tau_{\text{mean}}$ $\phi_T$
5 mM $\text{Mg}^{2+}$						
Nonphosphorylated						
$\tau_c$	2.497	1.190	0.189	0.052		2.096
$A_{\text{exp}}$	0.37	0.27	0.16	0.20		—
$\phi_c$	23.0	8.0	0.75	0.26		32.0
Phosphorylated						
$\tau_c$	2.492	1.179	0.242	0.070		2.051
$A_{\text{exp}}$	0.30	0.23	0.19	0.28		—
$\phi_c$	17.2	6.25	1.06	0.45		25.0
2 mM $\text{Mg}^{2+}$						
Nonphosphorylated						
$\tau_c$	2.458	1.133	0.170	0.053		2.063
$A_{\text{exp}}$	0.36	0.24	0.19	0.21		—
$\phi_c$	20.5	6.3	0.75	0.27		27.8
Phosphorylated						
$\tau_c$	2.311	0.969	0.270	0.071		1.627
$A_{\text{exp}}$	0.16	0.19	0.26	0.39		—
$\phi_c$	8.4	4.2	1.59	0.63		14.8

transition. The main change at  $F_0$  is the decrease in state 2 of the yield of the 500 ps decay, which is the reason for the slight decrease in the average lifetime. At  $F_M$  there is again no significant alteration in the  $\tau_c$  values, but the yield of the 2 ns decay component is decreased by 24% and there is an increase in the yields of the other three components on going to state 2.

Table III shows the effect of protein phosphorylation at 5 and 2 mM  $Mg^{2+}$  on the individual decay components at  $F_M$ . At 5 mM  $Mg^{2+}$  the phosphorylation does not significantly change the  $\tau_c$  values, except perhaps an increase from 189 to 242 ps in the second rapid decay after phosphorylation. It can be seen that the main difference between the nonphosphorylated and phosphorylated thylakoids is in the phosphorylation-induced decrease in the yield of the two long-lived components and the increase in the yield of the two rapid decays. Phosphorylation at 2 mM  $Mg^{2+}$  leads to a slight decrease in the lifetimes of the longer-lived decays and a continued increase in the lifetime of the '200 ps' component, from 170 to 270 ps. The additional fluorescence quenching due to phosphorylation

seen at 2 mM  $Mg^{2+}$  with respect to 5 mM  $Mg^{2+}$  is mainly due to the further decrease in the yield of the longest decay component, while the two fast components show a further increase in yield.

Table IV shows the effect of the presence (5 mM) and the absence of  $Mg^{2+}$  on the four individual decay components at both  $F_0$  and  $F_M$ . It can be seen that the absence of  $Mg^{2+}$  lowers the  $F_0$  level, decreases the yield of each individual decay and increases the lifetime of the slowest decay component. At  $F_M$ , however, large differences can be seen. The absence of  $Mg^{2+}$  appears to lead to a decrease in the lifetime of both slow components (2.61 to 1.905 ns and 1.27 to 0.835 ns) and in their yields, whereas the yield and lifetime of the '200–300 ps' decay increases (228 to 277 ps). The yield of the fastest decay component is also decreased in the absence of  $Mg^{2+}$ .

Fig. 4 shows the effect of PS II trap closure (as depicted from the average lifetime, which is proportional to the fluorescence yield, see Fig. 2) on the  $\tau_c$  values in the absence of  $Mg^{2+}$ . The changes in the two long-lived components appear to be almost parallel with the  $y$ -intercept of the longest decay at 800 ps. Another variable component is

TABLE IV

COMPONENT LIFETIME (ns), AMPLITUDE ( $A_{exp}$  (%)) AND FLUORESCENCE YIELD (REL. UNITS), AVERAGE LIFETIME ( $\tau_{mean}$  (ns)) AND TOTAL FLUORESCENCE YIELD (REL. UNITS) EXHIBITED BY LETTUCE CHLOROPLASTS AT  $F_0$  AND  $F_M$  IN THE PRESENCE (5 mM) AND ABSENCE OF  $Mg^{2+}$

Condition	Component characteristics				$\frac{\tau_{\text{mean}}}{\phi_{\text{T}}}$
No Mg <sup>2+</sup>					
F <sub>0</sub>					
τ <sub>c</sub>	1.198	0.354	0.139	0.050	0.292
<i>A</i> <sub>exp</sub>	0.01	0.15	0.44	0.39	–
φ <sub>c</sub>	1.18	5.21	6.00	1.91	14.30
F <sub>M</sub>					
τ <sub>c</sub>	1.905	0.835	0.277	0.050	0.974
<i>A</i> <sub>exp</sub>	0.08	0.29	0.31	0.32	–
φ <sub>c</sub>	7.10	11.28	8.06	1.50	46.60
5 mM Mg <sup>2+</sup>					
F <sub>0</sub>					
τ <sub>c</sub>	0.863	0.360	0.155	0.040	0.323
<i>A</i> <sub>exp</sub>	0.02	0.22	0.25	0.51	–
φ <sub>c</sub>	2.04	9.36	4.58	2.41	18.40
F <sub>M</sub>					
τ <sub>c</sub>	2.610	1.270	0.228	0.040	1.886
<i>A</i> <sub>exp</sub>	0.16	0.27	0.16	0.41	–
φ <sub>c</sub>	55.14	45.28	4.82	2.17	107.40

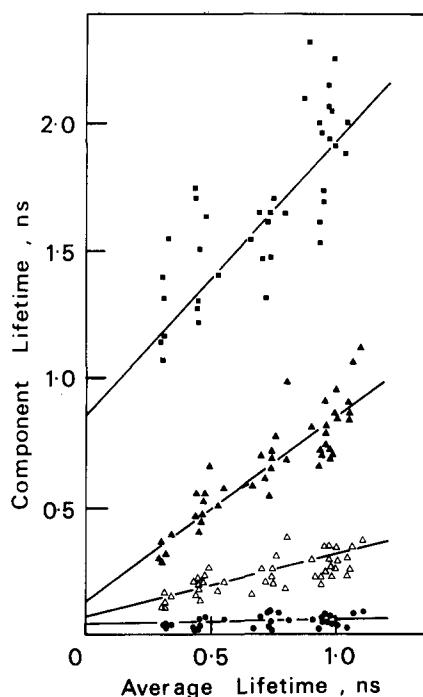


Fig. 4. The effect of PS II trap closure, as measured by average fluorescence lifetime (ns), on the lifetimes of the four individual kinetic decay components of the overall fluorescence decay exhibited by thylakoids of lettuce suspended in the absence of  $\text{Mg}^{2+}$ . The lines are the least-squares fit to all the datum points.

also seen ( $\tau = 150\text{--}350$  ps). The yield of each variable decay component also increases on closing PS II reaction centres, while the rapid component's yield decrease slightly (see Table 4). Fig. 5 shows the effect of PS II trap closure on the  $\tau_c$  values exhibited by thylakoids suspended in the presence of 5 mM  $\text{Mg}^{2+}$ . It can be seen that the longest-lived component behaves differently from in the minus  $\text{Mg}^{2+}$  situation, in that it does not parallel the change in the 300–1200 ps decay. Secondly, the '200 ps' decay does not give rise to a variable lifetime. The changes depicted in Fig. 5 are very similar to those already reported for algae [26], as are the changes in component yield (not shown).

## Discussion

### State 1–state 2 transition

A transition from state 1 to state 2 brings about an 18% decrease in the  $F_M$  (Table I), which can be

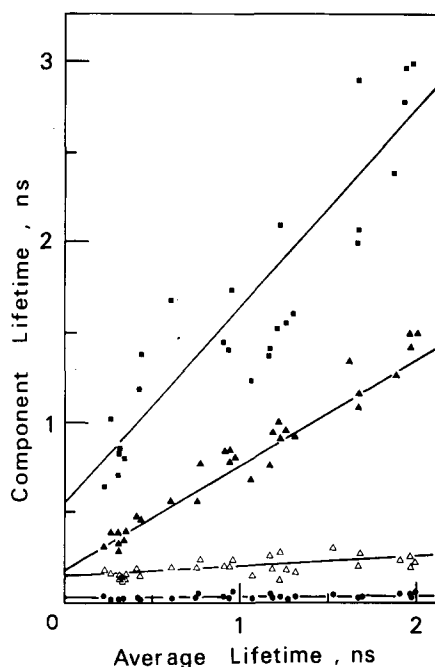


Fig. 5. The effect of PS II trap closure, as measured by average fluorescence lifetime (ns), on the lifetimes of the four individual kinetic decay components of the overall fluorescence decay exhibited by lettuce thylakoids suspended in the presence of 5 mM  $\text{Mg}^{2+}$ . The lines are the least-squares fit to all datum points.

due to a decrease in the absorption cross-section of PS II or to an increased deactivation of the excitation energy by spillover or heat. The small increase in the dinitrobenzene interaction index (Fig. 3) suggests only a small increase in the competition between dinitrobenzene and the 'normal' deactivation pathways, and therefore infers that most of the fluorescence quenching arises from a decrease in PS II absorption cross-section; this is also suggested from the change in the slope ( $\alpha$ ) seen in Fig. 1(A) and Table I. This small change in interaction index was not seen by Jennings and co-workers [32], who found a 15% decrease in the interaction index on going from state 1 to state 2. They therefore concluded that the state transition involved two types of quenching and proposed that it was brought about by both a change in PS II absorption cross-section and spillover. The changes seen in this work are very similar to those already reported in Ref. 11 for protein phosphorylation at 5 mM  $\text{Mg}^{2+}$ . The difference between our results and those of Jennings

and co workers might be explained by differences arising from growth conditions or species of *Chlorella* which could favour different energy redistribution mechanisms. As most of the room temperature fluorescence comes from PS II-associated pigments (less than 10% comes from PS I at  $F_M$  (see Ref. 25)) and as each PS II emission gives rise to variable fluorescence [26], then the 'global' analysis of the lifetime and yield (Figs. 1 and 2) are still valid. The analysis carried out in this work for the state transition (Fig. 1(A) and Table I) confirms the conclusion that most of the redistribution of excitation energy arises from a decrease in PS II absorption cross-section. This is also seen by the inability of the state 1–state 2 transition to alter the lifetimes of the individual kinetic components (Table II). The decrease in the yield of the 500 ps decay (at  $F_0$ ) and the 2 ns component (at  $F_M$ ) each by approx. 24% infers that it is the 500 ps decay which gives rise to the 2 ns decay on going from  $F_0$  to  $F_M$ . This conclusion is contrary to that put forward by Holzwarth and co-workers [24,27], in which the 500 ps decay arises from PS II $\beta$  centres and the 2 ns component is due to PS II $\alpha$ . At  $F_M$  the rapid (40–70 ps) component arises from PS I, and therefore the increase in the yield of this component in state 2 strongly suggests that more excitation energy is arriving at PS I. The decrease in average lifetime (Table II) and interaction index (Fig. 3) can therefore be explained by an increased competition between the dinitrobenzene and PS I to quench the excitation energy located in the phosphorylated LHC II. Furthermore, the decrease in the yield of the 2 ns component strongly suggests that it has LHC II origins.

#### Protein phosphorylation

The changes on the global level and on the individual kinetic component level brought about by the state 1–state 2 transition are very similar to those seen in vitro after protein phosphorylation at 5 mM  $Mg^{2+}$ . From the global analysis it appears that all of the fluorescence quenching due to phosphorylation at 5 mM  $Mg^{2+}$  can be accommodated by a decrease in PS II absorption cross-section (Table I and Fig. 1(B)). Protein phosphorylation at 5 mM  $Mg^{2+}$ , like the state transition, does not alter the lifetimes of the individual kinetic components (Table III), again suggesting

that the mechanism involves alterations in PS II absorption cross-section. It can be seen that at  $F_M$  in pea thylakoids that phosphorylation lowers the yield of the two long-lived components by approx. 24%, while increasing the yields of the two rapid decays. These changes can be interpreted by a decrease in PS II absorption cross-section and the subsequent increase in excitation energy arriving at PS I. Therefore, it seems that the 2.5 and 1.2 ns decay components both originate from LHC II if the well-established mechanism of protein phosphorylation (see Ref. 2) is correct, and therefore suggests a heterogeneous pool of LHC II (see Ref. 33). The slight difference between the state transition case and phosphorylation at 5 mM  $Mg^{2+}$  could be simply explained by the different species involved and the conditions used to bring about the organisational changes.

At 2 mM  $Mg^{2+}$  the phosphorylation increases the degree of fluorescence quenching, not by a further decrease in PS II absorption cross-section (see Table I) but by a change in the processes which lower the average fluorescence lifetime. This conclusion is in close agreement with other reports on the cation dependence of phosphorylation [9–11], carried out using steady-state fluorescence measurements. The changes observed by phosphorylation at 2 mM  $Mg^{2+}$  involve a small decrease in the lifetimes of the long-lived components which are not really large enough to explain a significant increase in spillover from PS II to PS I, although under these conditions the thylakoids are almost totally destacked [10]. The additional fluorescence quenching appears to be due to a continued decrease in the yield of the longest-lived component, with a very small decrease in lifetime. These changes suggest an additional change in absorption cross-section, which is not seen from Table I. This discrepancy could arise from the inability to resolve all of the individual kinetic components in a very heterogeneous system which could involve connected PS II–LHC II, PS II–LHC–PS I, phosphorylated LHC II–PS I, PS I, etc. An important conclusion, however, is that the changes in component lifetimes and the large quenching of the yields of long-lived components and the high increase in the rapid decays yields are not representative of the changes brought about by the state transition.



### Magnesium effect

Although the phosphorylation at 2 mM  $\text{Mg}^{2+}$  has been shown to lead to almost complete thylakoid destacking [10], similar to that seen in the absence of  $\text{Mg}^{2+}$ , the changes in the fluorescence lifetime parameters are not identical. On the global level it can be seen that the absence of  $\text{Mg}^{2+}$  leads to a quenching of chlorophyll fluorescence (57%), of which only 17% can be attributed to a decrease in PS II absorption cross-section (Table I). Meanwhile, Table IV shows that the individual lifetime components are not drastically affected with respect to component lifetime at  $F_0$  and only at  $F_M$  is there a significant decrease in the lifetimes of the slower components and an increase in the lifetime of the '200 ps' decay (Table IV). It is the yields of the individual components which are greatly altered, as the case of phosphorylation at 2 mM  $\text{Mg}^{2+}$ . These changes are again difficult to explain if the absence of  $\text{Mg}^{2+}$  leads to a large increase in spillover from PS II to PS I or an increased dissipation of energy by heat (as suggested from Fig. 2 and Table I), unless the long-lived component seen in the absence of  $\text{Mg}^{2+}$  is not the same as that observed in the presence of  $\text{Mg}^{2+}$ . This interpretation is borne out by a comparison between Figs. 4 and 5, in which the characteristics of the longest-lived decay component on closing PS II are different in the two cases. We suggest that the slow component in the absence of  $\text{Mg}^{2+}$ , due to its characteristics, arises from a small pool of poorly connected LHC II and that it is different in nature to the long-lived component seen in the presence of 5 mM  $\text{Mg}^{2+}$ . The component (350–835 ps) in the absence of  $\text{Mg}^{2+}$  might represent the slow component at 5 mM  $\text{Mg}^{2+}$  after a quenching of approx. 50%. The variable component (140–280 ps) seen in the absence of  $\text{Mg}^{2+}$  could therefore correspond to the plus  $\text{Mg}^{2+}$  decay (360–1270 ps) after a similar quenching, superimposed on the rapid constant PS I emissions. Furthermore, the dynamic nature of the components on closing PS II (Fig. 4) suggests that even in the absence of  $\text{Mg}^{2+}$  there rests some connection between PS II reaction centres which is not distinguished from the analysis of induction curves.

### Conclusions

(1) The state 1–state 2 transition is brought about mainly by a decrease in PS II absorption cross-section and a subsequent increase in PS I excitation which is comparable to protein phosphorylation at 5 mM  $\text{Mg}^{2+}$  carried out on isolated thylakoids.

(2) Only a minority of the fluorescence quenching provoked by the absence of  $\text{Mg}^{2+}$  is due to a diminished PS II absorption cross-section, while the majority arises from an increase in spillover (or internal dissipation).

(3) Even in the absence of  $\text{Mg}^{2+}$  there remains a partial connectivity between PS II reaction centres, although this situation gives rise to an exponential fluorescence induction rise.

(4) The changes observed suggest that the two long-lived decay components have LHC II origins and that it is the 500 ps component at  $F_0$  which gives rise to the 2 ns component at  $F_M$ , and not the 200 ps decay as proposed in Refs. 24 and 27.

(5) There is no need to evoke the  $\alpha/\beta$  heterogeneity to explain the changes brought about by phosphorylation or the state transition as described in Refs. 19 and 24.

### Acknowledgements

M.H. would like to thank the Royal Society (London, U.K.) for financial support. This work has also been supported by the CNRS. We are indebted to Dr. K.K. Rao (King's College, London, U.K.) for his generous gift of *Spirulina maxima* ferredoxin and D. Guyon for the upkeep of the *Chlorella pyrenoidasa*.

### References

- 1 Bonaventura, C. and Myers, J. (1969) *Biochim. Biophys. Acta* 189, 366–383
- 2 Barber, J. (1986) in *Photosynthetic mechanisms and the Environment, Topics in Photosynthesis*, Vol. 6 (Barber, J. and Baker, N.R., eds.), pp. 91–134, Elsevier Science Publishers, Amsterdam
- 3 Barber, J. (1976) in *The Intact Chloroplast, Topics in Photosynthesis*, Vol. 1 (Barber, J., ed.), pp. 88–134, Elsevier, Amsterdam
- 4 Allen, J.F., Bennett, J., Steinback, K.E. and Arntzen, C.J. (1981) *Nature* 291, 21–25
- 5 Bennett, J. (1983) *Biochem. J.* 212, 1–13

- 6 Saito, K., Williams, W.P., Allen, J.F. and Bennett, J. (1983) *Biochim. Biophys. Acta* 724, 94–103
- 7 Kyle, D.J., Haworth, P. and Arntzen, C.J. (1982) *Biochim. Biophys. Acta* 680, 336–342
- 8 Horton, P. and Black, M.T. (1983) *Biochim. Biophys. Acta* 722, 214–218
- 9 Telfer, A., Hodges, M. and Barber, J. (1983) *Biochim. Biophys. Acta* 725, 167–175
- 10 Telfer, A., Hodges, M., Millner, P.A. and Barber, J. (1984) *Biochim. Biophys. Acta* 766, 554–562
- 11 Hodges, M. and Barber, J. (1984) *Biochim. Biophys. Acta* 767, 102–107
- 12 Vernotte, C., Briantais, J.-M., Armond, P. and Arntzen, C.J. (1975) *Plant Sci. Lett.* 4, 115–123
- 13 Malkin, S., Telfer, A. and Barber, J. (1986) *Biochim. Biophys. Acta* 848, 48–57
- 14 Canaani, O., Barber, J. and Malkin, S. (1984) *Proc. Natl. Acad. Sci. USA* 81, 1614–1618
- 15 Bennoun, P. (1974) *Biochim. Biophys. Acta* 368, 141–147
- 16 Bennoun, P. and Jupin, H. (1974) in 3rd International Congress on Photosynthesis (Avron, M., ed.), pp. 163–169, Elsevier, Amsterdam
- 17 Wollman, F.-A. and Delepelaire, P. (1984) *J. Cell Biol.* 98, 1–7
- 18 Haworth, P., Karukstis, K.K. and Sauer, K. (1983) *Biochim. Biophys. Acta* 725, 261–271
- 19 Berens, S.J., Scheele, J., Butler, W.L. and Madge, D. (1985) *Photochem. Photobiol.* 42, 51–57
- 20 Nairn, J.A., Haehnel, W., Reisberg, P. and Sauer, K. (1982) *Biochim. Biophys. Acta* 682, 420–429
- 21 Karukstis, K.K. and Sauer, K. (1985) *Biochim. Biophys. Acta* 806, 374–388
- 22 Moya, I., Govindjee, Vernotte, C. and Briantais, J.-M. (1977) *FEBS Lett.* 75, 13–18
- 23 Moya, I., Sebban, P. and Haehnel, W. (1986) in *Light Emission by Plants and Bacteria* (Govindjee, Ames, J. and Form, D.C., eds.), pp. 161–190, Academic Press, New York
- 24 Holzwarth, A.R. (1986) *Photochem. Photobiol.* 43, 707–725
- 25 Hodges, M. and Moya, I. (1986) *Biochim. Biophys. Acta* 849, 193–202
- 26 Hodges, M., Moya, I., Briantais, J.-M. and Remy, R. (1986) in *Progress in Photosynthesis Research* (Biggins, J., ed.), Vol. I, pp. 115–118, Martinus Nijhoff, Dordrecht
- 27 Holzwarth, A.R., Wendler, J. and Haehnel, W. (1985) *Biochim. Biophys. Acta* 807, 155–167
- 28 Nakatani, H.Y. and Barber, J. (1977) *Biochim. Biophys. Acta* 461, 510–512
- 29 Moya, I., Hodges, M. and Barbet, J.-C. (1986) *FEBS Lett.* 198, 256–262
- 30 Vernotte, C., Briantais, J.-M. and Maisson-Peteri, B. (1982) *Biochim. Biophys. Acta* 681, 11–14
- 31 Jennings, R.C., Garalaski, F.M. and Gerola, P.D. (1983) *Biochim. Biophys. Acta* 722, 144–149
- 32 Jennings, R.C., Garalaski, F.M. and Zucchelli, G. (1986) in *Ion Interaction in Energy Transport Systems* (Papageorgiou, G., Barber, J. and Papa, S., eds.), pp. 223–236, Plenum Press, New York
- 33 Larsson, U.K., Sundby, C. and Andersson, B. (1986) in *Progress in Photosynthesis Research* (Biggins, J., ed.), Vol. II, pp. 677–680, Martinus Nijhoff, Dordrecht